ChemComm

Accepted Manuscript

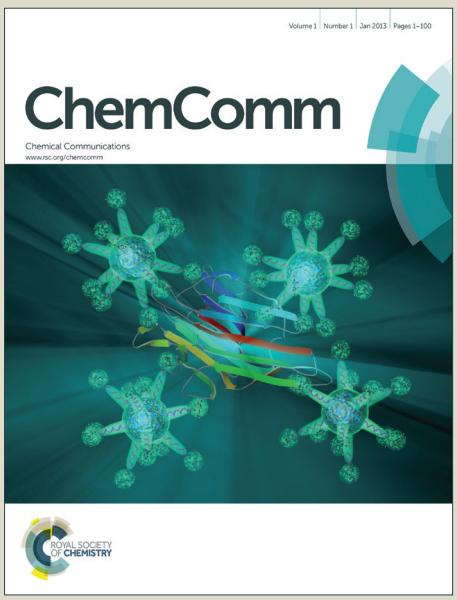

ROYAL SOCIETY OF CHEMISTRY

www.rsc.org/chemcomm

Journal Name

RSCPublishing

COMMUNICATION

Synthesis of Monolayer Platinum Nanosheets

Cite this: DOI: 10.1039/x0xx00000x

A. Funatsu,[a,b*] H. Tateishi,[a,b] K. Hatakeyama,[a,b] Y. Fukunaga,[a] T. Taniguchi,[a,b] M. Koinuma,[a,b] H. Matsuura,[a] and Y. Matsumoto[a,b]

Received 00th January 2012,
Accepted 00th January 2012

DOI: 10.1039/x0xx00000x

www.rsc.org/

Platinum (Pt) nanosheets were developed by exfoliating layered platinum oxide. Moreover, monolayer Pt nanosheets were succeeded for the first time in synthesizing by adjusting the conditions for reduction. Monolayer Pt nanosheets were highly active in oxygen reduction reaction.

Nanostructured materials exhibit many properties distinct from bulk materials owing to high surface-to-volume ratio and alteration in the electronic states. Unique nanosize effects such as quantum effects,[1)] surface plasmon resonance,[2)] and metastable phase stabilization[3)] have significantly contributed to rapid progress in nanoscience and nanotechnology.

Two-dimensional (2D) nanosheets possess unusual physical[4)] and chemical[5)] properties due to strong 2D quantum and surface effects. The emergence of graphene,[4)] which has high surface area, has remarkably accelerated the development of nanosheet-based devices and has revealed unique features of ultrathin nanosheets.

Pt-based materials have attracted considerable attention due to the superior performance of Pt in applications such as catalysis[6)], hydrogen production[7)], fuel cells[8)], and sensors.[9)] To address the increasing demand for Pt in the context of limited supply, maximizing the utilization efficiency of Pt is of importance. Recent efforts to improve the utilization efficiency have been directed toward tuning specific structural features of Pt nanostructures to produce catalysts with high surface area, and consequently, to achieve superior catalytic performance.

The synthesis of Pt-based nanomaterials with a controlled structure and morphology or surface area is expected to lead to their use in new applications. Examples of Pt-based nanostructures include dendritic Pt nanoparticles,[10)] Pt nanosheets with a nanogroove-network structure,[11)] three-dimensional porous Pt nanosheets,[12)] Pt nanotubes and nanoflowers,[13)] and Pt–Cu nansheets.[14)] A few researchers have studied layered Pt-based nanosheets; Shirai et al have reported the synthesis of Pt nanosheets between graphite layer.[15)-16)] However, Pt nanosheets were scarcely maintainable without supports and no investigations of monolayer Pt-based nanosheets have been reported.

Here we report the preparation of monolayer Pt nanosheets with homogeneous thickness by the exfoliation of layered Pt precursor materials with the addition of sodium dodecyl sulfate (SDS) during precursor preparation employing electrochemical reduction. Nanostructured Pt has attracted widespread attention owing to its use in fuel cell catalysis. Monolayer Pt nanosheets will prove essential for new nanodevices, such as nanocells, and will further the investigation of the characteristics of electrochemical reactions.

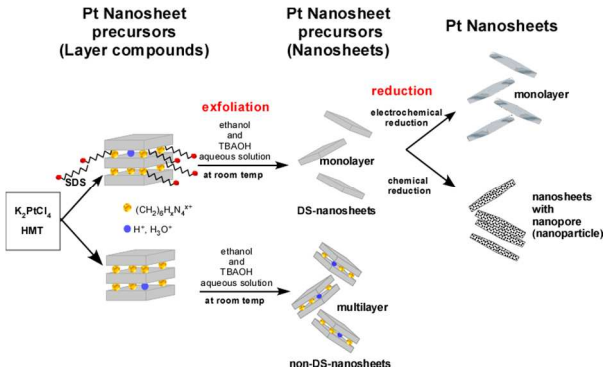

Scheme 1 Illustration of synthesis of monolayer Pt nanosheets

Scheme 1 illustrates the steps involved in the preparation of monolayer Pt nanosheets. The Pt nanosheets have two-step precursors, i.e., layered compounds and nanosheets. The nanosheet precursors were prepared in the presence and absence of SDS. The two types of layered compounds were synthesized by mixing an aqueous solution of K_2PtCl_4, hexamethylenetetramine (HMT), and SDS as follows. Aqueous (deionized-water) solutions of K_2PtCl_4, SDS, and HMT were mixed in 100 cm^3 vessels. The mixtures were allowed to sit for 24 h at room temperature. Subsequently, the mixtures were centrifuged. The precipitates were rinsed with distilled water and ethanol and then dried at room temperature. Each precipitated layered compound was exfoliated in ethanol and tetrabutylammonium hydroxide (TBAOH) aqueous solutions. Furthermore, the Pt nanosheet precursors were subsequently reduced either chemically or electrochemically; thus, two types of Pt nanosheets were synthesized.

Fig. 1a shows the X-ray diffraction (XRD) patterns for the layered compounds. Both layered compositions have several (00n) reflections labelled with asterisks. The basal spacings calculated from the reflection angles are 1.2 nm, independent of the presence of

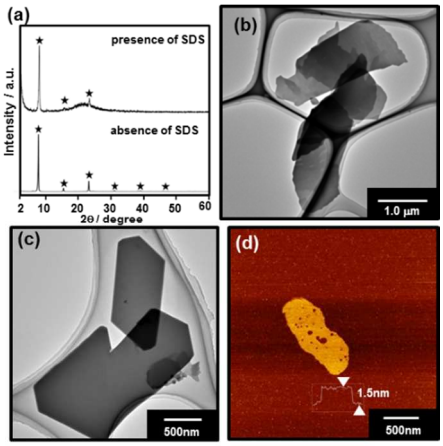

Fig. 1(a) XRD patterns of layer compounds in the presence and absence of SDS. TEM image of a DS nanosheets (b) and non-DS nanosheets(c). (d) AFM images of a DS nanosheets.

SDS during the synthesis process. Fig. S-1 shows scanning electron microscopy images layered compositions (both in the presence and absence of SDS). Some layered structures were observed. According to the X-ray photoelectron spectroscopy (XPS) analyses (Table S-1), the S/Pt ratio (in the case of SDS addition), and the K/Pt and, Na/Pt ratios were less than 0.1, indicating that the concentration of DS ions and alkali metal ions in the interlayers was very low. In contrast, there was a significant amount of N in the samples; N/Pt was greater than 7.0. The large inter-layer spacing indicates that the presence of interlaced $(CH_2)_6H_xN_{4x}^+$ between nanosheet layers. In fact, HMT provides OH^- by hydrolysis, as shown in Eq. 1.[17] Then, the Pt^{2+} in the solution reacts with the produced OH^- to form Pt(OH) (or $PtO{\bullet}nH_2O$) nuclei through Eq. 2.

$$(CH_2)_6N_4 + x\,H_2O \rightarrow (CH_2)_6H_xN_4^{x+} + xOH^- \quad \cdots \text{Eq. 1}$$

$$[PtCl_4]^{2-} + 2OH^- \rightarrow \underset{(PtO\cdot 2H_2O)}{Pt(OH)_2} + 4Cl^- \quad \cdots \text{Eq. 2}$$

To better understand the in-plane sheet-structure of the novel layered compound, we have performed selected area electron diffraction (SAED) analysis (see Fig. S-2). The SAED pattern from a typical plate-like product displayed halo ring patterns, indicating that the layered compound composed of many grains oriented in a random fashion. However, considering the well-defined edge structure of the products in Fig. 1c, the plate-like products might exhibit a single crystalline structure. Therefore, we cannot exclude that electron-beam irradiation decomposed the initial single crystal structure to nucleate nanocrystals. Thus, we think that the hallo ring patterns may not correspond to the real structure of as-obtained layered materials. Nevertheless, the hallo ring patterns corresponded well to a PtO phase with (tetragonal structure) so that the Pt-layer could exhibit a PtO-related structure. In addition, XPS indicates that the main oxidation state of Pt is divalent in the layered compositions (both in the presence and absence of SDS), as shown Table S-1. In addition, based on thermal analysis, some water molecules existed in the interlayers together with H^+ ions (as H_3O^+), as shown in Fig. S-3. Though the detailed structure and thermodynamic stability of the Pt-based novel layered material have not been identified yet, these results strongly suggest that Pt-layer include a Pt-O framework ($PtO \cdot nH_2O$).

In general, DS ions intercalate into interlayers during solution processing; [18] however, DS ions did not intercalate in the present case. The presence of DS ions in the reaction mixture results in the formation of tight layer compounds, as shown in Fig. S-1. The formation of tight layers resulted in monolayer nanosheets because layered compounds, i.e., densely stacked nanosheets, are easily synthesized in aqueous solutions, as will be discussed in a subsequent section. The DS ions will interact with layered PtO materials and somewhat suppress the crystallization of the layered compounds during the solution process, leading to the formation of monolayer nanosheets.

In this study, the nanosheets exfoliated from a DS-intercalated layered compound and a non-DS-intercalated layered compound are denoted as DS-nanosheets and non-DS-nanosheets, respectively. DS-nanosheets and non-DS-nanosheets were exfoliated from the layered compounds using a two-step method involving ethanol and an aqueous TBAOH solution. The concentration of Pt in the nanosheet solution was 2.1×10^{-4} M. Fig. 1b and 1c shows transmission electron microscopy (TEM) images of DS-nanosheets and non-DS-nanosheets, respectively. In Fig. 1c, a large plate was observed, possibly due to the nanoscale thickness of a small number of stacked monolayers. In Fig. 1b, small sheets were observed. In other words, these images indicate that the non-DS-nanosheets are multilayered nanosheets, while the DS-nanosheets are monolayered nanosheets. In fact, the DS-nanosheets were more easily exfoliated than non-DS-nanosheets due to the DS-nanosheets precursors. In addition, to prepare samples for atomic force microscopy (AFM) analysis, the obtained nanosheets were deposited on a mica substrate by casting. Fig. 1d shows AFM images of the DS-nanosheets. The thickness of DS-nanosheets was ca. 1.5 nm. Furthermore Fig. S-4 shows AFM images of the non-DS-nanosheets.

Next, the influence of the reduction approach was evaluated. In this study, we compared chemical and electrochemical approaches using a DS-nanosheet as the monolayer Pt nanosheet precursors (see Supplementary Information). The morphology and crystal structure of the nanosheets were studied by TEM. Fig. 2a shows a TEM image of DS-nanosheets after electrochemical reduction. A sheet type was observed. An AFM image of DS-nanosheets after electrochemical reduction is shown in Fig. 2b and Fig. S-5. AFM observation confirmed the presence of a sheet-type shape with a thickness of ca. 1.0 nm. In fact, the DS-nanosheets after electrochemical reduction indicates monolayer nanosheets because the atomic structure of the sheets is not destroyed during the reduction process.

A TEM image of the DS-nanosheets after chemical reduction is shown in Fig. 2c. Nanosheets with a nanopore structure, consisting of a nanoparticle assembly, were observed. The size of the nanoparticles ranged from ca. 1 to 3 nm (Fig. S-6). This sample revealed nanosheets but not monolayer nanosheets (Fig. S-7). Note that the shape of the obtained DS-nanosheets was dependent on reduction conditions. In other words, we succeeded in synthesizing monolayer Pt nanosheets only by electrochemical reduction.

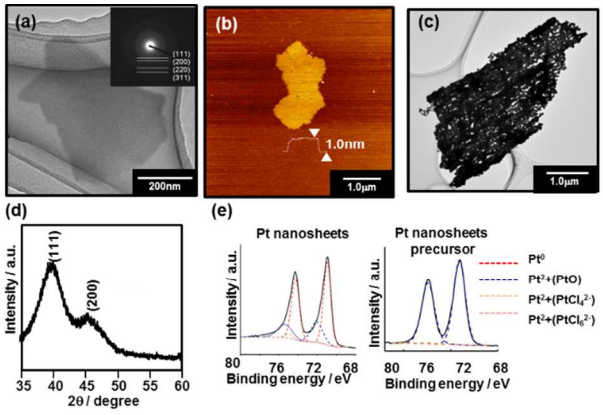

Fig. 2 (a) TEM image of a DS-nanosheets after electrochemical reduction. (b) AFM image of a DS-nanosheets after electrochemical reduction. (c) TEM image of a DS-nanosheets after chemical reduction. (d) XRD pattern of a DS-nanosheets after electrochemical reduction. (e) XPS spectra of the Pt 4f signal for the as-synthesized Pt nanosheets and Pt nanosheet precursors.

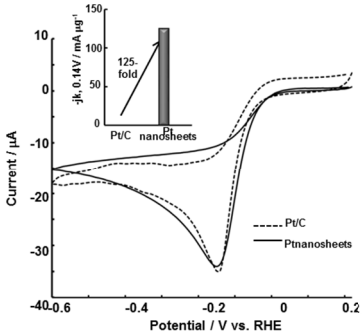

Fig. 3 CV curves of the monolayer Pt nanosheets and Pt/C on glassy carbon electrodes in O_2 -saturated 0.1 M KOH and mass-specific activities of Pt nanosheets and Pt/C for the ORR at 0.14 V in 0.1 M KOH.

To further confirm Pt formation, several other analytic methods, such as XRD, SAED pattern analysis, and XPS were also conducted. The XRD pattern of the monolayer Pt nanosheets (DS-nanosheets after electrochemical reduction) exhibited a face-centered cubic phase of Pt with a lattice constant a = 0.391 nm (JCPDS 04-0802), as shown in Fig. 2d. The SAED pattern revealed several bright concentric rings, which are attributed to (111), (200), (220), and (311) planes for the Pt phase (inset in Fig. 2a). The chemical state of Pt in the as-obtained nanosheets was checked by XPS.[19] The Pt 4f spectra of the Pt nanosheets and Pt nanosheet precursors are shown in Fig. 2e. The peaks at 71.0, 72.1, 73.0, and 75.0 correspond to the $Pt4f_{7/2}$ peaks of Pt^0, Pt^{2+}(PtO), Pt^{2+}($PtCl_4^{2-}$), and Pt^{4+}($PtCl_6^{4-}$), respectively. The peaks at 74.3, 75.4, 76.3, and 78.3 eV correspond to the $Pt4f_{7/2}$ peaks of Pt^0, Pt^{2+}(PtO), Pt^{2+}($PtCl_4^{2-}$), and Pt^{4+}($PtCl_6^{2-}$), respectively. As a result, most nanosheets demonstrate metallic Pt^0 species characteristics. In fact, the valence change of the reaction for

$$\underset{\text{Starting materials}}{[Pt^{2+}Cl_4]^{2-}} \rightarrow \underset{\substack{\text{Pt nanosheet precursors} \\ \text{(Layer compounds or nanosheets)}}}{Pt^{2+}O} \rightarrow \underset{\text{Pt nanosheets}}{Pt^0} \qquad \cdots \text{ Eq. 3}$$

Pt nanosheets preparation was expressed as described in Eq. 3.

To assess the validity of monolayer Pt nanosheets as an electrocatalyst, the oxygen reduction reaction (ORR) activity of the monolayer Pt nanosheets was examined by cyclic voltammetry (CV).[20] CV measurements were recorded in an O_2-saturated 0.1 M KOH solution. The electrode was prepared by casting GC substrates into a DS-nanosheet suspension and dried at room temperature. Then electrochemically reduced at −1.0 V (Ag/AgCl) for 3600 sec. Commercial 20wt % platinum on Vulcan carbon black was used as the reference electrode. This result agrees with monolayer Pt nanosheet have higher ORR activity as well as that of the commercial Pt/C. In addition, the mass specific activities of these samples at 0.14 V were compared inset in Fig. 3, which shows that Pt nanosheets were c.a. 125-fold significantly more active than Pt/C (Fig. S-8)[21]. Thus, the formation of monolayer nanosheets with high surface area enabled the production of excellent ORR properties. Furthermore we found that DS-nanosheet after chemical reduction have the ORR activity, too (Fig. S-9 and S-10).

Nanosheets have a geometric advantage over other types of structured nanomaterials because highly oriented films can be easily grown by stacking techniques[22] moreover, it is also possible to fabricate hybrid materials using various nanosheets as building blocks. Therefore, heterogeneous catalysis using Pt nanosheets can have a potentially important role in many applications.

Conclusions

Pt nanosheets were developed by exfoliating layered PtO materials after electrochemical reduction. Moreover, we succeeded in synthesizing monolayer Pt nanosheets by adjusting reduction conditions. Monolayer Pt nanosheets exhibited high ORR activity. To the best of our knowledge, this study represents the first report of monolayer Pt nanosheets. The electrochemical activity of these monolayer Pt nanosheets supports their use as fuel cell catalysts.

Notes and references

[a] Graduate School of Science and Technology, Kumamoto University, 2-39-1 Kurokami, Chuo-ku, Kumamoto 860-8555, Japan. E-mail: yasumi@gpo.kumamoto-u.ac.jp; afunatsu@kumadai.jp. Fax: +81-96-342-3679; Tel: +81-96-342-3659.

[b] Japan Science and Technology Agency (JST), CREST, K's Gobancho, 7, Gobancho, Chiyoda-ku, Tokyo 102-0075, Japan.

Electronic supplementary information (ESI) available: Experimental details, TG, SEM images, TEM images, AFM images, Binding energy values of the main peaks in the XPS spectra of Pt nanosheets and nanosheet precursors. See DOI: 10.1039/c000000x/

1. F. L. Kavan, M. Kalba M. Zukalova´ I' Exnar, *Chem. Mater.* 2004, **16**, 477-485
2. L. Lu, A. Kobayashi, K. Tawa, Y. Ozaki, *Chem. Mater.* 2006**, 18,** 4894-4901
3. G. M-Ribeiro, T. I. Kamins, D. A. A. Ohlberg, R. S. Williams, *Phys. Rev. B 1998, **58***, 3533-3536.
4. A. K. Geim, K. S. Novoselov, *Nat. Mater,* 2007, **6**, 183-191.
5. (a) F. Geng, R. Ma, A. Nakamura, K. Akatsuka, Y. Ebina, Y. Yamauchi. N. Miyamoto, Y. Tateyama, T. Sasaki, Nat. Commun, 2013, 4, 1632-1638. (b) R. E. Schaak, T. E. Mallouk, Chem. Mater, 2000, 12, 2513-2516.
6. (a) T. S. Ahmadi, Z. L. Wang, T.C. Green, A. Henglein, M. A. El-Sayed, *Science* 1996, **272**, 1924-1926. (b) C. Wang, H. Daimon, T. Onodera, T. Koda, S. Sun, *Angew. Chem. Int. Ed.* 2008, 47, 3588-3591
7. B. Seger, P. V. Kamat, *J. Phys. Chem. C* 2009, **113**, 18946-18952
8. H.A. Gasteiger, S.S. Kocha, B. Sompalli, F.T. Wagner, *Appl. Catal. B Environ.* 2005*,* **56**, 9–35
9. A. Chen, P. Holt-Hindle, *Chem. Rev.* 2010, **110**, 3767–3804
10. L. Wang, Y. Yamauchi, *J. Am. Chem. Soc.* 2009, **131**, 9152−9153.
11. G. Sakai, T. Y. shimura, S. Isohata, M. Uota, H. Kawasaki, T. Kuwahara, D. Fujikawa, and T. Kijima, *Adv. Mater*, 2007, **19**, 237-241.
12. X. Tong, G. Zhao, M. Liu, T. Cao, L. Liu, P. Li, *J. Phys. Chem. C* 2009, **113**, 13787-13792
13. L. Su, W. Jia, L. Zhang, C. Beacham, H. Zhang, Y. Lei, *J. Phys. Chem. C* 2010, **114**, 18121-18125
14. Y. Jia, Y. Jiang, J. Zhang, L. Zhang, Q. Chen, Z. Xie, L. Zheng, *J. Am. Chem. Soc.* 2014, **136**, 3748-3751
15. M. Shirai, K. Igeta, M. Arai, Chem. Comm. 2000, 623-624
16. L. Su, W. Jia, L. Zhang, C. Beacham, H. Zhang, Y. Lei, *J. Phys. Chem. C* 2010, **114**, 18121-18125
17. (a) S. Wang, Y. Zhao, J. Chen, R. Xu, L. Luo, S. Zhong, *Superlattices and Microstructures*, 2010, **47**, 597-605. (b) N. Iyi, T. Matsumoto,Y. Kaneko, K. Kitamura, *Chem. Lett.* 2004, **33**, 1122-1123.
18. S. Ida, D. Shiga, M. koinuma, and Y. Matsumoto, J. Am. Chem. Soc, 2008, **130**, 14038-14039.
19. T. Cochell, A. Manthiram, *Langmuir,* 2011, 1579−1587.
20. T. Taniguchi, H. Tateishi, S. Miyamoto, K. Hatakeyama , C. Ogata, A. Funatsu , S. Hayami , Y. Makinose, N. Matsushita Michio Koinuma , and Y Matsumoto, *Part. Part. Synst. Chract.* 2013, **30**, 1063-1070.
21. (a) R. R. Adzic, J. Zhang, K. Sasaki, M. B. Vukmirovic, M. Shao, J. X. Wang, A. U. Nilekar, J. A. Valerio, F. Uribe, *Top. Catal.* 2007, **46**, 249-262. (b) M. Shao, K. Shoemaker, A. Peles, K. Kaneko, L. Protsailo, *J. Am. Chem. Soc.* 2010, 132, 9253-9255
22. M. Osada, T. Sasaki, *Adv. Mater.* 2012, **24**, 210–228